

Electronic measurements of entropy in meso- and nanoscale systems

Eugenia Pyurbeeva,^{1, a)} Jan A. Mol,¹ and Pascal Gehring^{2, b)}

¹⁾*School of Physics and Astronomy, Queen Mary University of London, Mile End Road, London E1 4NS, UK*

²⁾*IMCN/NAPS, Université Catholique de Louvain (UCLouvain), 1348 Louvain-la-Neuve, Belgium*

(Dated: 14 June 2022)

Entropy is one of the most fundamental quantities in physics. For systems with few degrees of freedom, the value of entropy provides a powerful insight into its microscopic dynamics, such as the number, degeneracy and relative energies of electronic states, the value of spin, degree of localisation and entanglement, and the emergence of exotic states such as non-Abelian anyons. As the size of a system decreases, the conventional methods for measuring entropy, based on heat capacity, quickly become infeasible due to the requirement of increasingly accurate measurements of heat. Several methods to directly measure entropy of mesoscopic quantum systems have recently been developed. These methods use electronic measurements of charge, conductance and thermocurrent, rather than heat, and have been successfully applied to a wide range of systems, from quantum dots and molecules, to quantum Hall states and twisted bilayer graphene. In this Review, we provide an overview of electronic direct entropy measurement methods, discuss their theoretical background, compare their ranges of applicability and look into the directions for their future extensions and applications.

CONTENTS

I. Introduction	1
II. Alternative entropy measurements in continuous-charge nanodevices	2
A. Thermocurrent-based method for bulk materials	3
B. Maxwell relations for entropy measurements	3
C. Charge continuity assumptions	3
III. Quantised-charge nanodevices	4
A. The effects of charge quantisation	4
B. Degeneracy effects in electrical properties of nanodevices	5
C. Thermodynamic parameters of a quantised-charge system	5
D. Maxwell relations in quantised-charge systems	6
E. Quantised-charge entropy measurement methods	6
F. Limitations of entropy measurement methods	8
IV. Current applications	9
A. Detection of non-Abelian anyons.	9
B. Twisted bilayer graphene.	9
C. Single electron transistors	9
V. Discussion and Outlook	10
VI. Conclusion	11
VII. Acknowledgements	11

I. INTRODUCTION

The connection between macroscopic observables and microscopic dynamics was first made by Maxwell when he attributed part of the heat capacity C of a gas to the rotational degrees of freedom of its molecules¹. The name *entropy* was coined by Clausius in 1865 to describe the non-usable energy increase in a steam engine's exhaust as a function of its temperature T through the relation $dS = CdT/T$. Boltzmann and Gibbs later gave entropy its statistical basis that connects the observable averaged state functions to the microscopic dynamics of a system described by the number of microstates Ω and their probabilities, epitomised by Boltzmann's constant k_B in his definition of entropy $S = k_B \ln \Omega$. Since then, entropy measurements based on heat capacity and temperature have been used to probe the microscopic structure of bulk materials, such as the disorder in alloys²⁻⁴, phase transitions in molecular crystals⁵ and the magnetic arrangements of spin-ice⁶.

The development of nanofabrication, in particular molecular beam epitaxy and electron beam lithography, has made it possible to confine electrons in one or more dimensions. This has enabled the measurement of heat capacity and entropy in mesoscopic systems such as two-dimensional (2D) electron gasses in GaAs quantum well structures⁷⁻⁹ and of fractional quantum Hall systems^{10,11}. These experiments present significant difficulties as the contribution to the heat capacity of the confined electronic states is generally far smaller than that of the vibrations, or phonons, in the substrate material. To overcome this challenge, the electronic contribution to the heat capacity was increased by increasing the number of quantum wells⁷⁻⁹ and by exploiting the difference in thermalisation time of the electronic and phononic systems^{10,11}. Despite the ingenuity of these solutions, further down-scaling of entropy measurements based on heat capacity to few-electron nanodevices is practically impossible as the small numbers of electrons and electronic states involved require the measure-

^{a)}Electronic mail: e.d.pyurbeeva@qmul.ac.uk

^{b)}Electronic mail: pascal.gehring@uclouvain.be

ment of increasingly small amounts of heat, and heat capacities. For comparison, the maximum heat capacity of a single electronic spin is of the order of 10^{-24} J/K, while the minimal values of heat capacity per particle experimentally measured in¹¹ are three orders of magnitude greater.

Yet, it is precisely for a system containing only a few particles that entropy measurements can reveal the most about its microscopic dynamics. For example, the von Neumann entropy of the entangled state $(|00\rangle + |11\rangle)/\sqrt{2}$ is $k_B \ln 2$, while the entropy of the product state $(|00\rangle + |01\rangle + |10\rangle + |11\rangle)/2$ is zero^{12,13}. There is therefore a strong motivation to measure the entropy of few-electron quantum systems that has led to the development of alternative ways that do not rely on detecting the prohibitively small flow of heat. Electronic entropy measurements have recently emerged to address this challenge. Unlike heat, charge is a conserved quantity, which makes it much easier to measure. Charge sensitivities down to level of $10^{-6} \times e/\sqrt{\text{Hz}}$ can be achieved in few-electron devices, and charge currents as small as 10^4 e/s can be detected. Both these measures, of charge state and current, can be used to determine the entropy of a system. Electronic entropy measurements are thus ideally suited to probe microscopic dynamics of few-electron quantum systems that are weakly coupled to their environment.

This Review will summarize the thermodynamic theory underpinning both charge- and current-based entropy measurements of mesoscopic quantum systems, and discuss their application to several material systems and devices, including spin-ices and spin-frustrated systems⁶, twisted bilayer graphene^{14,15}, Kondo-systems¹⁶, quantum Hall states, and quantum dots and quantum dot systems^{17,18} as well as single-molecule devices^{19,20}. In all these systems electronic entropy measurements may serve a dual purpose. On the one hand, electronic entropy measurements provide insight into the internal quantum structure of matter, and might reveal exotic quasi-particles such as Majorana fermions. On the other hand, knowledge can be gained about the operation of an entire new class of nanoscale thermodynamic systems that include single-electron heat engines that operate close to the Curzon-Albhorn limit²¹, stochastic Maxwell demons^{22–24} and Szilard engines²⁵, and clocks^{26,27}.

Structure layout. This Review is structured as follows: first, in Section II we discuss the methods for measuring entropy through non-heat parameters in bulk materials, where charge, or particle number can be considered to be a continuous parameter. Then, in Section III we look into the change in the approach in the case of quantised charge, the methods proposed for this case and their limitations. Section IV is devoted to the performed experiments in entropy measurement and potential systems that would benefit from entropic research. Finally, in Section VI, we conclude with a discussion of the limitations of electronic entropy measurements and the directions in which we see them further developed.

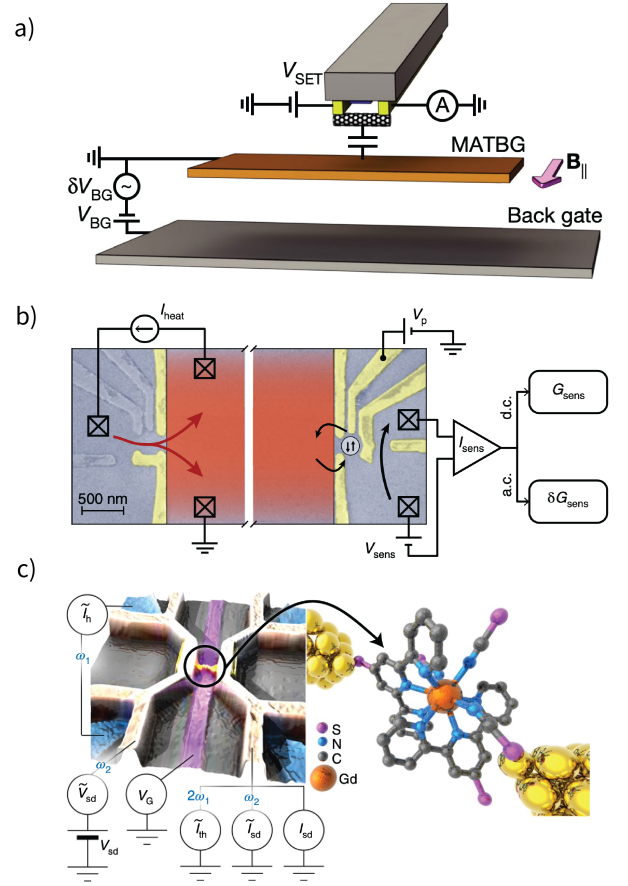


FIG. 1. Experimental setups for measuring entropy in nanoscale systems. a) A nanotube-based single electron transistor measuring the charge density and compressibility in a continuous-charge system (twisted magic-angle graphene)¹⁴. The graphene is encapsulated from both sides by insulating h-BN layers (not shown). The back gate is used for setting the chemical potential of the graphene. *Figure from*¹⁴ b) A charge-state based entropy measurement setup in a GaAs quantum dot¹⁷. The gold electrodes define the main quantum dot (red), a quantum point contact (QPC) of the left side of the device is used to control the temperature of the electron gas, while the QPC on the right is used as a charge sensor. *Figure from*¹⁷ c) A transport entropy measurement setup in a single-molecule device¹⁹. A molecule bridges the gap formed by electromigration of gold contacts. Each side of the device has a heater (blue), while the back-gate (purple) is used to control the energy levels of the molecule. Simultaneous measurement of current, conductance and thermocurrent is possible due to the double demodulation technique – the components of current through the molecule are taken at zero frequency, the oscillation frequency of the bias voltage and double the frequency of the heater bias. *Figure from*¹⁹

II. ALTERNATIVE ENTROPY MEASUREMENTS IN CONTINUOUS-CHARGE NANODEVICES

As was argued in the Introduction, the classical thermodynamic approach to measuring entropy is not suitable when the system size reaches mesoscopic or nanoscopic dimensions.

Therefore, when the size of the system decreases, other parameters could be measured from which the entropy can be determined, and that are easier to access in experiments than heat flows.

A. Thermocurrent-based method for bulk materials

The first example of utilising the connection between entropy and electric measurements comes from thermoelectrics – a field which by definition links heat (entropy) and charge transport. It has long been known that the Seebeck coefficient is a measure for the entropy per unit charge carrier²⁸.

For a free electron gas the low-temperature Seebeck coefficient (often referred to as thermopower) is directly proportional to the entropy of a unit charge carrier²⁹. This holds true in a wide range of bulk solid materials^{30,31}, where the Seebeck coefficient can be used to measure entropy, however does not apply to all materials. For instance, the relation between the Seebeck coefficient and entropy falls apart in systems with highly anisotropic transport³². Despite this, thermopower has been proposed as an entropic probe for non-Abelian states³³.

B. Maxwell relations for entropy measurements

Maxwell relations are a textbook source of thermodynamically justified connections between the derivatives of various quantities. It was first proposed by Cooper and Stern³⁴ to employ them for the observation of entropic signatures of non-Abelian quantum Hall states, as an alternative to the interferometry methods proposed at the time^{35–38}. The work³⁴ uses two Maxwell relations:

$$\left(\frac{\partial m}{\partial T}\right)_B = \left(\frac{\partial s}{\partial B}\right)_T \quad (1)$$

$$\left(\frac{\partial \mu}{\partial T}\right)_n = -\left(\frac{\partial s}{\partial n}\right)_T \quad (2)$$

where B and T are the magnetic field and temperature – free parameters for the experimentalist, m , n and μ are the magnetisation density, the electron surface density and the chemical potential – quantities that can be measured, and s is the entropy per unit area, which can reveal the non-Abelian degrees of freedom.

At the same time, nothing in equations 1 and 2 is specific to the quantum Hall effect. Indeed, the authors³⁴ suggest the application of the same Maxwell relation method to any electronic system with temperature- and field-dependent magnetisation, such as spin-ordering transitions in low density electron gases in the Wigner crystal or Luttinger liquid states. Additionally equations similar to 1 and 2 can be written for many parameters, to explore systems with different effects, such as pressure and volume or electric field and dipole moment.

Recently, two works^{14,15} have utilised the Maxwell relation approach to study magic-angle twisted bi-layer graphene and reveal a Pomeranchuk-type effect in it (see Section IV B): a

temperature and magnetic field-driven transition from a low-entropy electronic liquid to a state with nearly free magnetic moments and a high entropy. This has been achieved with a single-electron transistor close to the graphene stack (see Figure 1a), which was used to measure the local charge, related to n . The chemical potential μ was controlled by applying a gate voltage.

C. Charge continuity assumptions

Although Maxwell relations, like most thermodynamic methods, are system-independent, their application requires that the partial derivatives as well as the mean values of all parameters (magnetic moment, entropy and number of electrons per unit area or volume) are well-defined. This does not necessarily hold true in small systems. Indeed, the validity of the direct application of the Maxwell relation provides a qualitative distinction between two types of nanodevices, which we will call continuous-charge and quantised-charge.

The ability to include the mean magnetic moment, entropy or particle number in the derivatives in equations 1 and 2 mathematically requires them to have continuous values. The simplest quantity to consider is the mean particle number n . For any finite system, the number of particles it contains is quantised, and therefore so is the surface or volume particle density of the system. However, in Maxwell equations in classical macroscopic thermodynamics it is assumed that the number of particles is large enough that the quantisation of n is insignificant. This is equivalent to the statement that with the small change of particle number the properties of the system experience small changes, which are linear with the particle number change.

It is important to note that the same assumption is covertly made in the Seebeck coefficient approach (Section II A). Associating an entropy to every electron in a current is only possible if there is no large change of the entropy of the system depending on the exact number of electrons currently occupying it, as the presence of any particle flow is impossible without particle number fluctuations. Additionally, Maxwell or similar relations are used in the existing derivations of the exact equality between thermopower and entropy per unit charge^{28,31–33}.

Thus, all systems can be divided into continuous-charge ones, to which the approaches described in this section are applicable, and ones where a change in particle number leads to non-linear changes in other quantities – these we will call quantised-charge nanodevices.

In Figure 1 the twisted bilayer graphene sample (Fig. 1a) provides the example of a continuous-charge device, while the GaAs quantum dot (Fig. 1b) and the single-molecule device (Fig. 1c) are quantised-charge devices, which are the topic of discussion in the following section.

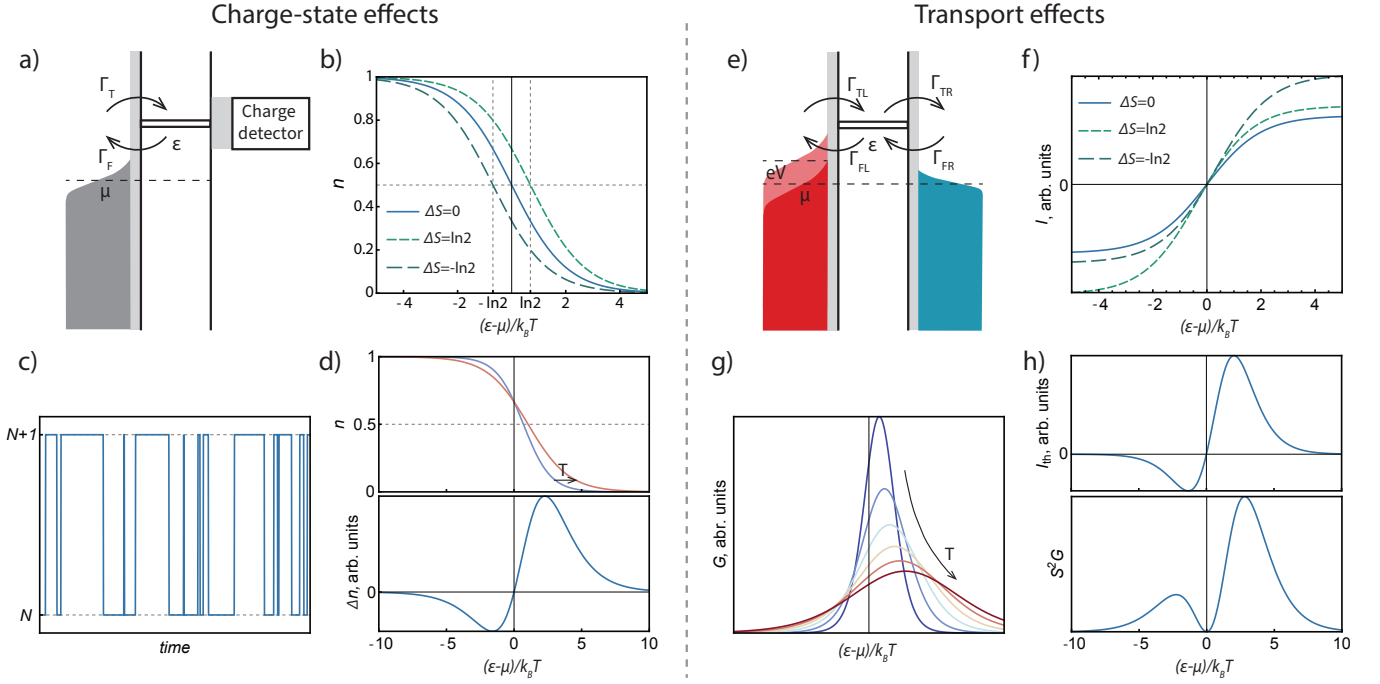


FIG. 2. Entropic effects in charge state and charge transport measurements in quantised-state nanodevices. a) A schematic of a charge state measurement setup. An energy level coupled to a thermal bath, with the charge state of the level independently determined. b) The mean excess population n of the energy level in the case of the non-degenerate and two-fold degenerate energy level ($\Delta S = 0$ or $\Delta S = \pm \ln 2$). c) A model of experimental time-resolved measurement of the charge state of the device. Information of entropy (or degeneracy) can be extracted from the proportion of time the device spends in each of the charge states³⁹. d) A model of the experiment performed in¹⁷ – mean population is measured as a function of gate voltage (energy level), where an overall shift of the distribution is observed on top of its spreading. The exact value of the entropy difference can be found from fitting the difference between the populations at the two temperatures. e) A schematic of a charge transport measurement setup. The energy level is coupled to two thermal baths, with a potential and/or a temperature difference across. The current through the system is measured. f) The current through the nanodevice for a non-degenerate and two-fold degenerate energy level ($\Delta S = 0$ or $\Delta S = \pm \ln 2$). g) A model of the experimental thermal shift of the conductance peak of a device, as observed in^{19,40}. h) A model of the thermocurrent and power factor measurement of a quantised-charge nanodevice. The value of the entropy difference can be extracted from the asymmetry.

III. QUANTISED-CHARGE NANODEVICES

A. The effects of charge quantisation

Quantised-charge nanodevices are those where the derivatives by particle number N can not be defined. One must note that a quantised-charge nanodevice does not necessarily contain a smaller total number of particles than a continuous-charge one. The difference lies in the number of available particle number states and the dependence of energy on them rather than the overall particle number. A well-defined derivative requires the existence of a linear approximation of energy as a function of particle number for several values of the latter.

The most common example of a system without a derivative by particle number are nanodevices in the state of Coulomb blockade⁴¹, where the electrostatic repulsion is the dominant energy scale and only few charge states (values of particle number in the system) are energetically allowed. Typical examples for such systems are quantum dots^{42,43} (see Figure 1b) and molecular devices in the weak coupling transport

regime^{44,45} (see Figure 1c).

In such devices, the electrostatic energy change with the increase of particle number depends on the particle number itself:

$$E_{el}(N+1) - E_{el}(N) = 2E_C \left(N + \frac{1}{2} - N_0 \right) \quad (3)$$

where E_{el} is the electrostatic energy, E_C is the charging energy with $E_C = e^2/C$, C is the system's capacitance, and N_0 is the induced charge, which is a function of gate voltage.

Thus, both a single molecule in the sequential tunnelling regime (Fig 1c) and a GaAs quantum dot with a characteristic size of hundreds of nanometer (Fig 1b) are quantised-charge nanodevices in the sense that derivatives by particle number cannot be defined in them, due to the significant electrostatic contribution to the energy, despite having vastly different overall numbers of electrons. A GaAs quantum dot, while being a quantised-charge device, might have more electrons in total than a given sample of magic-angle graphene in the continuous-charge regime (Fig 1a).

Most frequently, Coulomb-blocked devices are considered in the case where only two charge states are energetically available: N and $N + 1$. In this case no linearisation of any parameter by particle number can be justified, if N and $N + 1$ are the only two available charge states:

$$\left(\frac{\partial X}{\partial N}\right)_Y \neq \frac{X(N+1) - X(N)}{\Delta N} = X(N+1) - X(N) \quad (4)$$

where X is some variable. Additionally, the partial derivative at constant Y can not be defined, as each charge state is associated with its own value of Y . This means that the approach outlined in section II cannot be applied directly.

B. Degeneracy effects in electrical properties of nanodevices

The effects of transport level degeneracy on the electrical properties of Coulomb-blocked nanodevices have long been an area of study⁴⁶ with no connection to entropy. This degeneracy can originate from electron spin orientation and, in molecular devices, from orbital degeneracy^{47–49}.

Rate equation has been the standard approach to these systems, with the rates of particle exchange between the nanoscale system and an electron bath being described as⁵⁰:

$$\begin{cases} \Gamma_T = \gamma d_{N+1} f(\varepsilon) \\ \Gamma_F = \gamma d_N (1 - f(\varepsilon)) \end{cases} \quad (5)$$

where $\Gamma_{T/F}$ is the rate of electrons moving To/From the system, γ is the geometric coupling factor, $\varepsilon = E(N+1) - E(N)$ is the energy associated with the change of the charge state, $f(\varepsilon)$ is the Fermi-distribution, the occupation number in the bath at ε and finally, $d_{N/N+1}$ is the degeneracy of $N/N + 1$ charge state (See Fig 2a).

If the system is coupled to two baths (see Fig 2e), the rate equation takes a similar form, where the index L/R corresponds to the Left/Right bath being involved:

$$\begin{cases} \Gamma_{TL/R} = \gamma_{L/R} d_{N+1} f(\varepsilon_{L/R}) \\ \Gamma_{FL/R} = \gamma_{L/R} d_N (1 - f(\varepsilon_{L/R})) \end{cases} \quad (6)$$

The dependence of hopping rates on the charge state degeneracy affects both the mean population of the dot, $\langle N \rangle$, or $n = \langle N \rangle - N$, and its transport properties, as the charge state occupation probabilities

$$p_{N/N+1} = \frac{\Gamma_{F/T}}{\Gamma_T + \Gamma_F} \quad (7)$$

and the steady-state current

$$I = \Gamma_{TL} p_N - \Gamma_{FL} p_{N+1} = \Gamma_{FR} p_{N+1} - \Gamma_{TR} p_N \quad (8)$$

both depend on the rates and thus the degeneracies (see Fig. 2b for the population dependence and Fig. 2f for current).

Degeneracy effects of both types, static (charge) and dynamic (transport) have been experimentally observed. Hofmann et al.³⁹ performed a direct measurement of the charge

state of a quantum dot over time, using a quantum point contact situated close to the dot (see Figure 2c), showing the time it spends in each is related to the degeneracy.

The effects of degeneracy on charge transport include the shift of the conductance peak with temperature (see Figure 2g), predicted in⁴⁶ and measured in^{19,40}, the asymmetry of the thermocurrent and power factor peaks⁴⁰ (see Figure 2h) and, as was later shown in¹⁸, the effect of non-zero thermopower at the charge degeneracy point in the Coulomb Blockade valley^{51,52}.

Degeneracy effects in electric measurements of nanodevices can be used as a starting point towards entropy measurements. The degeneracy of a charge state is the number of equally probable microstates it contains. Thus, any effect allowing to discern degeneracy has the potential to be used in the more general case with unequal microstate probabilities. A common route to the derivation of an electronic entropy measurement method, is to start from a degeneracy effect and theoretically generalise it to apply to systems more complex than those having an integer number of equally probable microstates. However, before we move on to entropy measurements in quantised-charge nanodevices, we discuss their thermodynamic description.

C. Thermodynamic parameters of a quantised-charge system

One of the main strengths of thermodynamics is system-independence. The thermodynamic treatment of quantised-charge devices can allow for the development of entropy measurement methods that apply not only to devices with a single degenerate energy level, discussed in Section III B, but to those with more general dynamics.

It can be done in a way analogous to the continuous-charge regime, discussed in Section II: starting from thermodynamic principles and using Maxwell relations. However, to do this in quantised-charge systems, one has to specify the parameters used in the thermodynamic description of a small quantised-charge system, namely the temperature, chemical potential, particle number and entropy. Below, we treat them separately.

Temperature. While a quantised-charge system, or its electronic state dynamics may or may not be sufficiently large to have its own definable temperature, the Maxwell equation approach taken in section II requires equilibrium conditions. Following this, we may take the temperature of the nanoscale system to be equal to the well-defined temperature of the bath it exchanges electrons with^{12,53,54}. In the case of more than one bath being present, equilibrium is only possible when the temperature differences between the baths are infinitesimally small, and the temperature of the system can be defined to a small window.

Chemical potential. It is customary in the quantum dot community to call the energy difference between the charge states $U(N+1) - U(N)$ the chemical potential⁴². However, it does not agree with the canonical definition of the chemical potential:

$$\mu = \left(\frac{\partial U}{\partial N}\right)_S \neq \frac{U(N+1) - U(N)}{1}, \quad (9)$$

not only due to the absence of the derivative, but also as the effect that is studied in the dependence of entropy on charge state, thus changing the charge state at constant entropy is impossible.

Instead, for quantised-charge systems, one should take the approach similar to that of temperature^{20,55} – if a system is in equilibrium with a bath regarding particle exchange, its chemical potential is equal to that of the bath^{53,54}. And if several baths are present, for quasi-equilibrium conditions the difference in chemical potentials must be infinitesimally small.

For all realistic temperatures nanoelectronic measurements are performed, the electron gas is highly degenerate and the chemical potential is to a high degree of accuracy equal to the Fermi energy E_F .

Particle number. In the Coulomb-blocked state we consider, the system only allows two particle numbers, N and $N + 1$, and in the presence of particle exchange with the bath, the particle number is not only a function of external parameters (temperature, chemical potential, magnetic field, etc) as it is in the continuous case (section ??), but also of time. To simultaneously remove this dependence and large fluctuations $\Delta N = 1$ as well as the discontinuity, the mean number of particles can be used as a variable:

$$\langle N \rangle = p_N N + p_{N+1} (N + 1) = N + p_{N+1} \quad (10)$$

Here, one can define the “mean excess number of electrons” $n = p_{N+1}$, which changes between 0 and 1, as N remains constant in our consideration.

Entropy. In line with the mean particle number used in the thermodynamic description of quantised-charge nanodevices, which does not depend on time, one has to define entropy in a similar way, for a state with a given value of n . The entropy of a system in each of the charge states S_N or S_{N+1} is easily defined, however in the case of fluctuating charge, an additional term is needed to account for the uncertainty of the charge state itself. It can be shown that entropy in that case is equal to²⁰:

$$S = S_0 + n S_{N+1} + (1 - n) S_N \quad (11)$$

where S_0 is the “coarse-grained” Gibbs entropy of the charge state uncertainty $S_0 = -n \ln n - (1 - n) \ln(1 - n)$.

D. Maxwell relations in quantised-charge systems

Taking the considerations for the treatment of independent thermodynamic parameters outlined in Section III C, the standard Maxwell relation should be interpreted as

$$\left(\frac{\partial \mu_B}{\partial T} \right)_{\bar{N}} = - \left(\frac{\partial S}{\partial \bar{N}} \right)_T \quad (12)$$

where μ_B is the chemical potential of the bath, \bar{N} is the mean time-averaged population of the system and S is the Gibbs entropy incorporating both charge state uncertainty and the entropy of the charge states.

The mean free energy of the system can be expressed as:

$$\bar{F} = E(N) + \varepsilon n - TS \quad (13)$$

where $\varepsilon = E(N + 1) - E(N)$ is the energy of the transport level described in section III B, which can be experimentally varied by the application of gate voltage, V_G : $\varepsilon = \varepsilon_0 + \alpha V_G$, where α is the lever arm, quantifying the electrostatic coupling between the system and the gate electrode. Using this and the relation for the chemical potential $\mu = (\partial \bar{F} / \partial \bar{N})_T$, one arrives at:

$$\varepsilon - \mu = T \left(\frac{\partial S}{\partial \bar{N}} \right)_T \quad (14)$$

In a two-charge-state system all derivatives by \bar{N} can be replaced by those by n , since N is constant. Rewriting equation 14 in this way in conjunction with the two-state entropy expression (eq. 11), we arrive at the *Microscopic Maxwell Relation*²⁰:

$$\frac{\varepsilon - \mu}{T} = k_B \ln \frac{1 - n}{n} + \Delta S \quad (15)$$

This relation can be independently proven²⁰ starting from the Gibbs distribution. Another property of Equation 15 is that the population of a system with an entropy difference ΔS between the charge states is:

$$n = \frac{1}{1 + e^{\frac{\varepsilon - \mu - T \Delta S}{k_B T}}}, \quad (16)$$

which is a Fermi-distribution shifted by $T \Delta S$.

A different approach, one that can be called an *Integral Maxwell Relation* involves reformulating the Maxwell relation (equation 12) in the same sense of time-averaged particle number \bar{N} and the chemical potential of the bath as^{55–57}:

$$\Delta S_{\mu_1 \rightarrow \mu_2} = \int_{\mu_1}^{\mu_2} \frac{d\bar{N}}{dT} d\mu_B \quad (17)$$

The benefit of Equation 17 is that it is completely equivalent to the Maxwell relation and therefore holds true for all systems. It has to be noted, however, that in it S is the total entropy, with no distinction between the entropy due to the charge state uncertainty and the entropy of the pure charge states.

Thus, in order to find ΔS between the charge states, one has to shift μ_B (or, equivalently ε) from the point of a pure N charge state to that of a pure $N + 1$ charge state: in the approximation of only two states being available, from $-\infty$ to ∞ , but in reality between the two consecutive Coulomb-blocked regions.

E. Quantised-charge entropy measurement methods

Charge-state based measurements Entropy measurement protocols can be divided into two groups – those based on

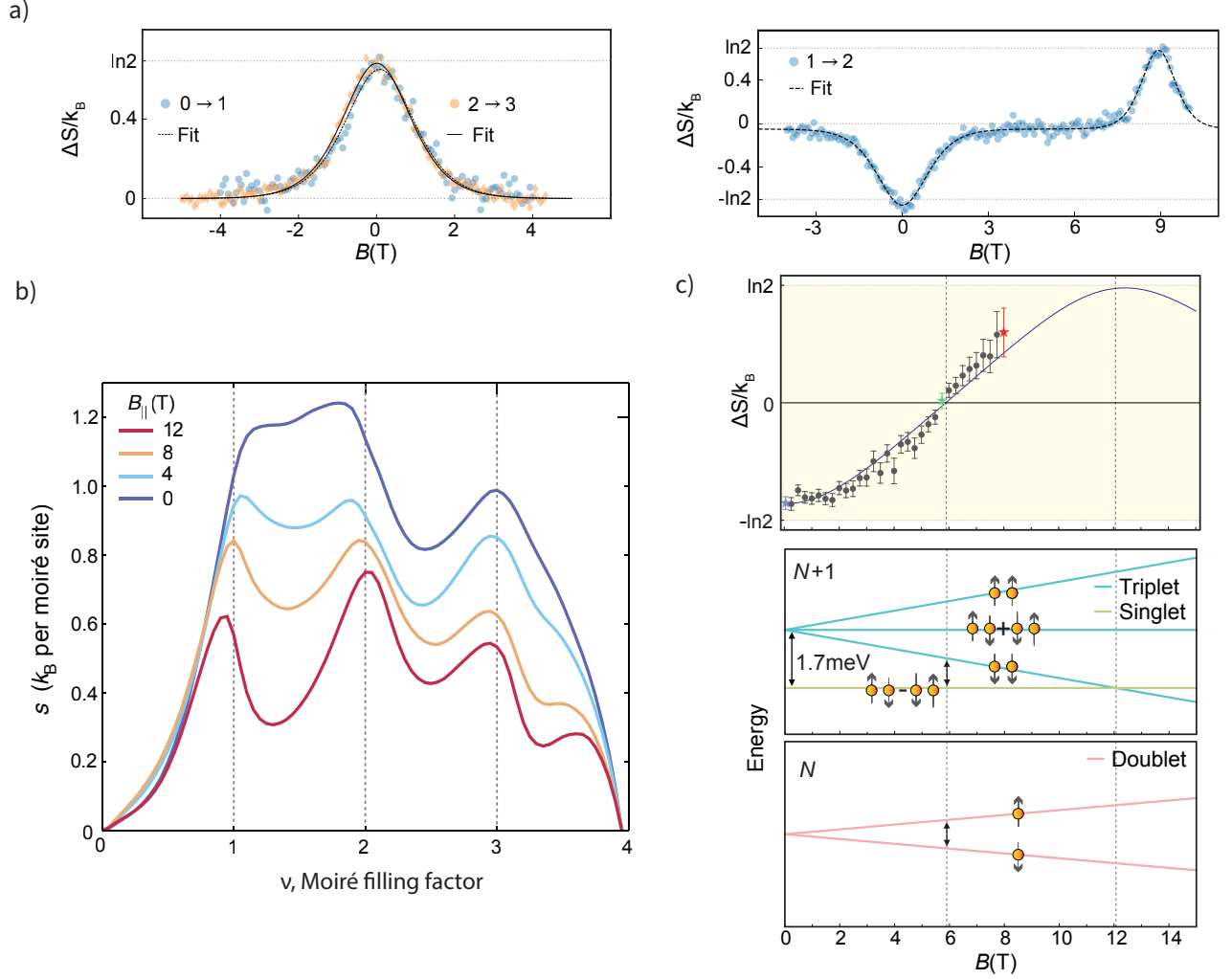


FIG. 3. a) Experimental results for the entropy difference between the N and $N + 1$ charge states as a function of magnetic field¹⁷ for two values of even (left) and on of odd (right) N . *Image modified from*¹⁷. b) The electronic entropy s of twisted bilayer graphene¹⁴ as a function of ν , the moiré lattice filling factor. *Image modified from*¹⁴. c) The entropy difference between two redox states of a single-radical molecule found through thermoelectric spectroscopy⁵⁸. The points in the top panel show the experimental data, while the solid line gives the fit to a doublet \leftrightarrow singlet + triplet transition model. The model parameters, such as the singlet-triplet splitting can be extracted from the fit.

charge state measurement and those based on charge transport.

The first proposed electronic entropy measurement method¹⁷ was a charge-state technique. It employed the thermal shift of the charge degeneracy ($n = 1/2$) point (see Fig 2b) as a measure for entropy difference between the charge states. A quantum point contact (QPC) was located close to a quantum dot in a GaAs lithographically-defined device and used as a mean charge sensor (Fig. 1b). The dependence of mean charge of the dot on the transport energy level was measured at two close temperatures, and the entropy difference was found by fitting the asymmetry of the difference curve (see Fig. 2d).

The energy of the level at which the probabilities of both charge states are equal, $\epsilon_{1/2}$, is related to temperature and the

entropy difference as:

$$\epsilon_{1/2} - \mu = T\Delta S \quad (18)$$

which gives the thermal shift:

$$\frac{\partial \epsilon_{1/2}}{\partial T} = \Delta S \quad (19)$$

In¹⁷, Equation 19 has only been proved for a degenerate level, however the same follows from equation 15 by substituting $n = 1/2$. The method described in¹⁷ has been applied to a quantum dot with a two-fold degenerate level, yielding $\Delta S = \ln 2$, and the same dot in a magnetic field (see Fig 3a).

Building on the first charge-state based entropy measurement method¹⁷, the theoretical applicability of the entropy

measurement method for the detection of Majorana zero modes has been demonstrated⁵⁶ (see Chapter IV A), by moving on to the integral Maxwell relation formulation.

Further developments concerned the design of a bespoke device and an optimised measurement protocol optimising thermal equilibration in the system⁵⁷, and the measurement of the entropy as a function of coupling strength (lifetime of a charge state), that could be controlled by gates forming the quantum dot⁵⁵.

Charge transport based measurements. The first charge transport entropy measurement protocol¹⁸ involves simultaneous measurement of conductance and thermocurrent and fitting the thermocurrent as:

$$L(\varepsilon, T) = C(T)L_{NI}(\mu + \Delta(T), T) + G(\mu, T)\frac{\Delta(T)}{T} \quad (20)$$

where L is the thermoelectric conductance $L = \partial I / \partial \Delta T$ of the device, L_{NI} is the thermoelectric conductance of the non-interacting (non-degenerate) level, which is symmetric in ε , G is the conductance and $\Delta(T)$ is a function of entropy such that $\partial \Delta(T) / \partial T = \Delta S / 2$.

Alternative charge transport entropy measurement protocols include observing the thermal shift of the conductance peak, proven in²⁰ and applied to a molecular device in¹⁹ (See Fig. 2g). For closely spaced energy levels $\delta \varepsilon \ll k_B T$ it can be shown²⁰ that the system population at the energy where the conductance peaks is equal to $1 - f(\varepsilon)$. Thus, substituting the population into equation 15, one arrives at:

$$\frac{\varepsilon_G - \mu}{T} = \frac{\Delta S}{2} \quad (21)$$

, where ε_G is the level energy for the charge peak. Or, for the thermal shift of the peak position:

$$\frac{\partial \varepsilon_G}{\partial T} = \frac{\Delta S}{2} \quad (22)$$

One has to note that, for general system dynamics $\varepsilon_{1/2} \neq \varepsilon_G$.

Each of the above two charge transport entropy measurement methods has its benefits and drawbacks. The fitting of thermocurrent and conductance using a symmetric non-interacting model¹⁸ requires the measurement of both thermocurrent and conductance simultaneously, and the model requires the use of two significant fitting parameters $C(T)$ and $\Delta(T)$. At the same time, the conductance peak shift method, while free of fitting parameters, requires measurements of the conductance at multiple temperatures, which is experimentally challenging due to the instability of nano-devices and the presence of charge traps.

Another transport-based entropy measurement method is described in⁵⁸, and called “thermocurrent spectroscopy”. It only requires the measurement of a thermocurrent trace recorded as a function of gate voltage, and used its asymmetry to find the entropy difference between the charge states (see Fig 2h).

Under small level spacing assumption, the thermocurrent trace can be described as:

$$L \sim \frac{\varepsilon}{T^2} [1 - f(\varepsilon)] f(\varepsilon - T \Delta S). \quad (23)$$

This method uses only one significant fitting parameter, ΔS , and requires a measurement at only a single temperature.

F. Limitations of entropy measurement methods

Both realisations of the Maxwell relation in microscopic systems (equations 15, 17) follow from the standard thermodynamic Maxwell relation and therefore apply to a wide range of systems. The most obvious group are those that can be represented by a set of arbitrarily spaced energy levels.

However, some physical properties of nanodevices are usually not considered in standard “macroscopic” thermodynamics. The two most obvious ones are vibrations and lifetime broadening.

It has been experimentally shown that mechanical degrees of freedom significantly affect charge transport in weakly coupled molecular devices^{48,59}. This was described by introducing a new energy parameter – the reconfiguration energy λ , which quantifies the energy that is lost to the phonon bath due to the relaxation performed by the molecule after an additional electron is added⁴⁹. This energy can be associated with an entropy change $\Delta S_{ph} = \lambda / T_{ph}$ of the phonon bath, where T_{ph} is its temperature. This is not a function of the state of the system because each of the charge states can not be attributed to a particular entropy due to the interaction between electronic and mechanical degrees of freedom and sources of entropy. Therefore, systems with vibrational effects are not described by the existing theory. At the same time, they offer a potential avenue of further work into electronic characterisation of mechanical states in systems with large electronic-mechanical coupling.

In the rate equation approach lifetime broadening is represented by a Lorentzian-shaped peak replacing the δ -function for the energy of the transport level⁴⁰. From the quantum-mechanical point of view, a finite electron lifetime in the charge states means that the number and energy operators, \hat{N} and \hat{E} , no longer commute. This invalidates the substitution of ε for μ_B in equation 15. However the integral form of the Maxwell relation (equation 17) appears to hold and the dependence of entropy on coupling strength (lifetime) has been experimentally measured⁵⁵. An interesting intuitive result⁵⁵ is that at high coupling strength (small lifetime) the entropy of a two-fold-degenerate quantum dot approaches the value of $\ln 3$, representing maximal uncertainty between “spin up”, “spin down” and “no extra electron” states.

Charge-transport based entropy measurement methods possess more limitations than the charge-state ones. Unlike mean charge, any transport property – conductance, thermocurrent, power factor, etc, is fundamentally a non-equilibrium quantity and therefore is not necessarily linked to entropy as a state function. Furthermore, the derivation of all existing charge transport entropy measurement methods assume small level splitting – a requirement that all energy states of the system observe the same electron population. This requirement was well-formulated in the SI to¹⁸: “one of the levels dominates the transport, or the levels are degenerate, or at high temperatures ($T \gg \delta \varepsilon$) or at low temperatures ($T \gg \delta \varepsilon$)”

IV. CURRENT APPLICATIONS

A. Detection of non-Abelian anyons.

Theoretical studies suggest that Majorana modes — fermions that are their own antiparticle — bear the potential to revolutionize quantum computing: Majorana qubits should support non-Abelian statistics, braiding and operate highly fault tolerant.⁶⁰ Particularly promising are propagating 1D Majorana modes as they enable ultra-fast quantum computation.⁶¹ Although several material systems have been predicted to host Majorana modes, their identification, and more importantly, their control is very challenging and scope of heavy ongoing research efforts. Most experiments focus on electrical fingerprinting, but a key drawback of this approach is, that the minute conductance signatures of Majorana modes could be easily misinterpreted or confused with non-Majorana mechanisms, especially in disordered samples.^{62–65} However, it has been predicted that entropy measurements could provide a robust signature of nonlocal Majorana zero mode (MZM) states^{34,66}: while a Majorana qubit – a nonlocal two-level system formed by two MZMs – has a trivial entropy of $k_B \ln 2$, a single MZM should possess an universal fractional entropy of $\frac{1}{2} k_B \ln 2$.⁶⁷

This could be measured by the temperature dependence of charge transitions using a local charge detector.^{17,56} Special care has then to be taken to reduce the finite coupling between two MZMs forming the Majorana qubit by either increasing their spatial separation or by controlling the tunneling phases of the MZMs⁶⁸ via, for example, local gates controlling the tunneling barriers between topological superconductors and quantum dots.^{69,70} Such experiments could be simplified by increasing the temperature, which diminishes the dependence of the entropy on the MZM tunneling phases, and by involving multiple MZMs. In the latter case the sensitive adjustment of the tunneling phases becomes obsolete and an entropy of $\frac{n}{2} k_B \ln 2$, where n is the number of MZMs, is expected.⁷¹

A single spin-1/2 impurity that is anti-ferromagnetically coupled to a single conduction electron channel can give rise to a *single channel Kondo* effect. Such Kondo effect is universal and its universality has recently been verified by thermocurrent spectroscopy⁷². At high temperatures the impurity is free and acts as an unpaired spin with entropy $k_B \ln 2$. At low temperatures the impurity is screened by the conduction electrons ("Kondo cloud"), and a many-body-singlet forms that has zero residual entropy. However, if there are multiple conduction electron channels the impurity can be "over-screened" and a finite residual entropy is expected. Depending on the exact number of channels such systems can host Majorana fermions (for two channels) with a residual impurity entropy of $k_B \ln \sqrt{2}$, or Fibonacci anyons with $k_B \ln \phi$, where $\phi = \frac{1}{2}(1 + \sqrt{5})$ is the golden ratio. A promising experimental realisation for the multi channel Kondo model are charge Kondo quantum dot devices^{73,74} for which it is predicted that non-Abelian anyons can be detected by entropy measurements.¹⁶

B. Twisted bilayer graphene.

Typically thermodynamic states with high entropy are more stable at higher temperatures than states with low entropy. As an example, a block of solid ice melts when heating it up. Curiously, in two recent experiments entropy measurements in twisted bilayer graphene^{14,15} have helped to discover an exotic phenomenon – the Pomeranchuk effect – that seemingly violates this intuitive picture. In both studies the change of the electrochemical potential μ of one-quarter-filled twisted bilayer graphene with temperature has been measured, either directly¹⁵, or by integrating the inverse local electronic compressibility measured by a nanotube-base scanning single electron transistor experiment¹⁴ (see Figure 1a). The entropy of the system could then be determined by using a Maxwell relation (see Equation 2). It was found that the entropy per electron of the electrically insulating phase that is observed at high temperatures is greater than that of the metallic phase found at low temperatures, by an amount that corresponds to that of a free electron's spin. From this it was concluded that the high-temperature insulating phase possesses ferromagnetic order with a low iso-spin (= combination of valley and spin degree of freedom) stiffness, which means that the iso-spins are globally aligned in one preferred direction but the constraint on their alignment is weak. On the other hand, in the metallic phase the constraint on iso-spin alignment is high to ensure a non-magnetic state and thus an equal number of iso-spins with opposite orientation. Consequently the slightly higher entropy of the ferromagnetic insulating state favours its stability at elevated temperatures. This transition – where electron spins freeze at higher temperature – is called a Pomeranchuk effect and was first discovered in liquid ³He which solidifies when increasing the temperature.

C. Single electron transistors

Single electron transistors – devices in which electrical transport is dictated by Coulomb repulsion and through which electrons flow consequently sequentially (one at a time) – have been realised in various systems, ranging from gate-defined quantum dots in semiconductor 2-dimensional electron gases⁷⁵, semiconductor nanostructures⁷⁶, heteronanowires⁷⁷ to single molecule junctions⁷⁸. Thanks to the countable number of charges on such devices, the theoretical framework presented in chapter III can be applied and the entropy of the system's few-electron ground states can be directly extracted from charge transport measurements.

To this end, the entropy of the first, second and third electron ground state in a GaAs quantum dot (Figure 3) has been measured by charge sensing (see Figure 1b)¹⁷. A precise value of $k_B \ln 2$ of a single spin 1/2 was found by studying the $N=0$ to $N=1$ charge transition. Furthermore, the entropy measurements allowed the authors to observe a singlet to triplet transition in the $N = 1$ to $N = 2$ transition at high magnetic fields (Figure 3). Such precise entropy measurements could be useful for probing more exotic systems like those with non-Abelian statistics (see Section IV A "Detection of non-

Abelian anyons").

The concept of using single molecules as building blocks of nanodevices is the core of ‘molecular electronics’ and gained enormous theoretical and experimental interest over the last decades. Because single molecules enable electronic devices at a length scale of 1-3 nm they offer the perfect platform for ultimate scaling and can surpass limitations of conventional silicon-based technologies⁷⁹. Furthermore, many studies have suggested that single molecules hold great potential for enabling applications in energy conversion and solid-state cooling. Thus, their thermoelectric investigation has received continuously growing attention in recent years^{79–84}. Theoretical simulations have shown that the thermoelectric figure of merit ZT can be significantly enhanced by engineering molecule length⁸⁵, optimizing the tunnel coupling strength of molecules via chemical anchor groups⁸⁶, or by quantum interference features in their transmission function⁸⁷. Furthermore, it has recently been suggested that molecular systems with highly degenerate ground states could lead to exceptionally high thermoelectric power factors.⁴⁹ Experimental studies on a Gd-terpyridine complex (see Figure 1c), where the spin-entropy of the molecular junction was extracted by conductance measurements as depicted in Figure 2g, could indeed show an enhancement of the power factor of the thermoelectric junction by spin entropy.¹⁹ Thermoelectric experiments on single-molecule junctions can furthermore serve as a novel kind of spectroscopy, which allows to extract useful information about the spin-ground state of the molecule. To this end, thermocurrent-spectroscopy experiments on a radical molecule⁵⁸ revealed that if a second electron is added to the radical molecule a singlet forms at low magnetic field while at higher magnetic fields the molecule is in a triplet ground state. This singlet-triplet transition could not be observed by using the charge transport data only, highlighting the power of thermocurrent-spectroscopy to quantify the entropy and spin configuration of single-molecular systems.

V. DISCUSSION AND OUTLOOK

We have discussed a group of methods that allow to determine entropy differences in a wide range of systems, from bilayer graphene to single molecules, through electric (or thermoelectric) means. Work on electronic entropy measurements started approximately fifteen years ago, but has taken off in the past five.

Currently, the existing methods are moving on from proof-of-concept experiments, measuring the entropy of a two-fold degenerate quantum dot (see Figure 3a)^{17,18} and conceptual theoretical work⁵⁶ to practical applications, such as the demonstration of a Pomeranchuk-type effect in twisted bilayer graphene^{14,15} (see Figure 3b) and finding the singlet-triplet transition energy in a single-molecule device (see Figure 3c). Work on improving experimental devices for greater accuracy is also ongoing⁵⁷.

As, and it is simply a matter of time, electronic entropy measurements complete the transition to yet another tool in the experimentalist’s toolbox, they will have two possible ap-

plications. First, as it is proposed for non-Abelian anyons (see Section IV A), measuring entropy can be an indirect signature for the presence of a particular effect, which may not be distinguishable by alternative means. Another approach is to use entropy measurements in order to determine microscopic dynamics, which was done to some extent in twisted bilayer graphene^{14,15} (Pomeranchuk effect allows to hypothesise on the magnetic interaction that would lead to it), and in a single-molecule device⁵⁸, where entropy measurements led to a full model of the energy level structure in a molecule.

The latter in particular solves a long-standing problem in molecular electronics, the ultimate goal of which is to utilise achievements in chemical synthesis in order to encode specific electric properties into molecules. The issue is that while standard spectroscopy techniques allow to find energy level structures in free molecules in a solution, it is largely unknown how coupling to metallic leads and incorporation into a solid-state device affects this structure. Thermoelectric spectroscopy allows to find the energy level structure directly in situ, especially if the model is known from standard measurements in a solution, and only the charges of parameters need to be determined.

A strength of transport-based entropy measurement methods is that they can be performed on devices that are otherwise widely studied, usually for thermoelectric research. In some cases^{47,88}, they can even be used as a post-factum analysis of existing experimental data.

Consideration of limitations of entropy measurement methods (Section III F) opens up new questions and areas of research. Examples of these include studying mechanical degrees of freedom in small systems with strong electron-vibrational coupling and electronic properties of devices in the rarely-considered intermediate case between the Landauer regime and weakly-coupled sequential tunnelling, in which lifetime in the device is small and has a significant contribution to entropy⁵⁵.

Finally, being able to measure thermodynamic parameters, primarily entropy, in nanodevices in which effects of stochastic, and especially quantum thermodynamics play a large role would allow to use nanodevices for experimental study of both. The usual approach taken experimentally is more bottom-up, including precise quantum manipulation of relatively few parameters and has been able to demonstrate the most unusual predictions of quantum thermodynamics⁸⁹. While such precision can not be achieved in electric nanodevices, they have the benefit of years of technological advancement for practical applications, and ease of experimentation.

The last application would require some theoretical work, as the term “open quantum systems” usually implies systems open to energy, but not particle exchange. However the experimental accessibility of electrical nanodevices which include both, unlike, for example, molecular rotors, can justify this effort.

VI. CONCLUSION

This review has examined the latest chapter in the long history of using entropy measurement as a macroscopic probe for microscopic dynamics. Unlike conventional entropy measurements that are based on measuring heat, these latest measurements probe entropy directly from charge and charge transport measurements in nanoelectronic devices. These electronic entropy measurements were first proposed in the early 2000s and have been experimentally demonstrated in the past few years. In this review we have attempted to develop a taxonomy for the different electronic measurement techniques, and reveal their underlying thermodynamic principles. To date, most effort has been on developing these novel measurement techniques, with demonstration of entropy measurements in a host of materials systems and devices. The next stage will be to apply these techniques in a systematic way to uncover microscopic dynamics of quantum correlated systems and potentially discover new and exotic quasi-particles in condensed matter systems. Much like heat-based measurements of entropy enabled the development of engines that powered a technological revolution in the 19th century, electronic measurements of entropy in meso- and nanoscale systems will power the quantum technology revolution of the 21st century.

VII. ACKNOWLEDGEMENTS

P.G. acknowledges financial support from the F.R.S.-FNRS of Belgium (FNRS-CQ-1.C044.21-SMARD, FNRS-CDR-J.0068.21-SMARD, FNRS-MIS-F.4523.22-TopoBrain), from the Federation Wallonie-Bruxelles through the ARC Grant No. 21/26-116 and from the EU (ERC-StG-10104144-MOUNTAIN). This project (40007563-CONNECT) has received funding from the FWO and F.R.S.-FNRS under the Excellence of Science (EOS) programme.

J.A.M. was supported through the UKRI Future Leaders Fellowship, Grant No. MR/S032541/1, with in-kind support from the Royal Academy of Engineering.

- ¹J. C. Maxwell, "II. Illustrations of the dynamical theory of gases," London, Edinburgh, Dublin Philos. Mag. J. Sci. **20**, 21–37 (1860).
- ²W. L. Bragg and E. J. Williams, "The effect of thermal agitation on atomic arrangement in alloys," Proc. R. Soc. London. Ser. A, Contain. Pap. a Math. Phys. Character **145**, 699–730 (1934).
- ³W. L. Bragg and E. J. Williams, "The effect of thermal agitation on atomic arrangement in alloys-III," Proc. R. Soc. London. Ser. A - Math. Phys. Sci. **152**, 231–252 (1935).
- ⁴F. C. Nix and W. Shockley, "Order-Disorder Transformations in Alloys," Rev. Mod. Phys. **10**, 1–71 (1938).
- ⁵G. B. Guthrie and J. P. McCullough, "Some observations on phase transformations in molecular crystals," J. Phys. Chem. Solids **18**, 53–61 (1961).
- ⁶A. P. Ramirez, A. Hayashi, R. J. Cava, R. Siddharthan, and B. S. Shastry, "Zero-point entropy in 'spin ice'," Nature **399**, 333–335 (1999).
- ⁷E. Gornik, R. Lassnig, G. Strasser, H. L. Störmer, A. C. Gossard, and W. Wiegmann, "Specific heat of two-dimensional electrons in GaAs-GaAlAs multilayers," Phys. Rev. Lett. **54**, 1820–1823 (1985).
- ⁸J. K. Wang, J. H. Campbell, D. C. Tsui, and A. Y. Cho, "Heat capacity of the two-dimensional electron gas in GaAs/Al_xGa_{1-x}As multiple-quantum-well structures," Phys. Rev. B **38**, 6174–6184 (1988).
- ⁹V. Bayot, E. Grivei, S. Melinte, M. B. Santos, and M. Shayegan, "Giant low temperature heat capacity of GaAs quantum wells near Landau level filling $\nu = 1$," Phys. Rev. Lett. **76**, 4584–4587 (1996).
- ¹⁰F. Schulze-Wischeler, U. Zeitler, C. v. Zobelitz, F. Hohls, D. Reuter, A. D. Wieck, H. Frahm, and R. J. Haug, "Measurement of the specific heat of a fractional quantum Hall system," Phys. Rev. B **76**, 153311 (2007).
- ¹¹B. A. Schmidt, K. Bennaceur, S. Gaucher, G. Gervais, L. N. Pfeiffer, and K. W. West, "Specific heat and entropy of fractional quantum Hall states in the second Landau level," Phys. Rev. B **95**, 1–5 (2017), arXiv:1605.02344.
- ¹²P. P. Potts, "Introduction to Quantum Thermodynamics," Tech. Rep., arXiv:1906.07439v1.
- ¹³R. Kosloff, "Quantum Thermodynamics: A Dynamical Viewpoint," Entropy **15**, 2100–2128 (2013), arXiv:arXiv:1305.2268v1.
- ¹⁴A. Rozen, J. M. Park, U. Zondiner, Y. Cao, D. Rodan-Legrain, T. Taniguchi, K. Watanabe, Y. Oreg, A. Stern, E. Berg, P. Jarillo-Herrero, and S. Ilani, "Entropic evidence for a pomeranchuk effect in magic-angle graphene," Nature **592**, 214–219 (2021).
- ¹⁵Y. Saito, F. Yang, J. Ge, X. Liu, T. Taniguchi, K. Watanabe, J. I. A. Li, E. Berg, and A. F. Young, "Isospin pomeranchuk effect in twisted bilayer graphene," Nature **592**, 220–224 (2021).
- ¹⁶C. Han, A. K. Mitchell, Z. Iftikhar, Y. Kleorin, A. Anthore, F. Pierre, Y. Meir, and E. Sela, "Fractional entropy of multichannel Kondo systems from conductance-charge relations," **2** (2021), arXiv:2108.12878.
- ¹⁷N. Hartman, C. Olsen, S. Lüscher, M. Samani, S. Fallahi, G. C. Gardner, M. Manfra, and J. Folk, "Direct entropy measurement in a mesoscopic quantum system," Nature Physics **14**, 1083–1086 (2018).
- ¹⁸Y. Kleorin, H. Thierschmann, H. Buhmann, A. Georges, L. W. Molenkamp, and Y. Meir, "How to measure the entropy of a mesoscopic system via thermoelectric transport," Nat. Commun. **10**, 5801 (2019), arXiv:1904.08948.
- ¹⁹P. Gehring, J. K. Sowa, C. Hsu, J. de Bruijckere, M. van der Star, J. J. Le Roy, L. Bogani, E. M. Gauger, and H. S. J. van der Zant, "Complete mapping of the thermoelectric properties of a single molecule," Nat. Nanotechnol. **16**, 426–430 (2021).
- ²⁰E. Pyurbeeva and J. A. Mol, "A Thermodynamic Approach to Measuring Entropy in a Few-Electron Nanodevice," Entropy **23**, 640 (2021), arXiv:2008.05747.
- ²¹M. Josefsson, A. Svilans, A. M. Burke, E. A. Hoffmann, S. Fahlvik, C. Thelander, M. Leijnse, and H. Linke, "A quantum-dot heat engine operating close to the thermodynamic efficiency limits," Nat. Nanotechnol. **13**, 920–924 (2018).
- ²²J. V. Koski, A. Kutvonen, I. M. Khaymovich, T. Ala-Nissila, and J. P. Pekola, "On-Chip Maxwell's Demon as an Information-Powered Refrigerator," (2015), 10.1103/PhysRevLett.115.260602.
- ²³R. Sánchez, P. Samuelsson, and P. P. Potts, "Autonomous conversion of information to work in quantum dots," **1**–18 (2019), arXiv:1907.02866.
- ²⁴R. Sánchez, J. Splettstoesser, and R. S. Whitney, "Nonequilibrium System as a Demon," Phys. Rev. Lett. **123**, 216801 (2019), arXiv:1811.02453.
- ²⁵S. W. Kim, T. Sagawa, S. De Liberato, and M. Ueda, "Quantum Szilard Engine," PRL **106**, 70401 (2011).
- ²⁶P. Erker, M. T. Mitchison, R. Silva, M. P. Woods, N. Brunner, and M. Huber, "Autonomous Quantum Clocks: Does Thermodynamics Limit Our Ability to Measure Time?" Phys. Rev. X **7**, 031022 (2017), arXiv:1609.06704.
- ²⁷A. N. Pearson, Y. Guryanova, P. Erker, E. A. Laird, G. A. D. Briggs, M. Huber, and N. Ares, "Measuring the Thermodynamic Cost of Timekeeping," Phys. Rev. X **11**, 021029 (2021), arXiv:2006.08670.
- ²⁸P. M. Chaikin and G. Beni, "Thermopower in the correlated hopping regime," Phys. Rev. B **13**, 647–651 (1976).
- ²⁹C. Goupil, H. Ouerdane, K. Zabrocki, W. Seifert, N. F. Hinsche, and E. Müller, "Thermodynamics and Thermoelectricity," in *Contin. Theory and Modeling Thermoelectr. Elem.* (Wiley, 2016) pp. 1–74.
- ³⁰K. Behnia, D. Jaccard, and J. Flouquet, "On the thermoelectricity of correlated electrons in the zero-temperature limit," J. Phys. Condens. Matter **16**, 5187–5198 (2004), arXiv:0405030 [cond-mat].
- ³¹V. Zlatić, R. Monnier, J. K. Freericks, and K. W. Becker, "Relationship between the thermopower and entropy of strongly correlated electron systems," Phys. Rev. B - Condens. Matter Mater. Phys. **76**, 1–16 (2007), arXiv:0512288 [cond-mat].
- ³²J. Mravlje and A. Georges, "Thermopower and Entropy: Lessons from Sr₂RuO₄," Phys. Rev. Lett. **117**, 036401 (2016), arXiv:1504.03860.

- ³³K. Yang and B. I. Halperin, “Thermopower as a possible probe of non-Abelian quasiparticle statistics in fractional quantum Hall liquids,” *Phys. Rev. B - Condens. Matter Mater. Phys.* **79**, 1–5 (2009), arXiv:0901.1429.
- ³⁴N. R. Cooper and A. Stern, “Observable bulk signatures of Non-Abelian quantum hall states,” *Phys. Rev. Lett.* **102**, 1–4 (2009), arXiv:0812.3387.
- ³⁵S. D. Sarma, M. Freedman, and C. Nayak, “Topologically protected qubits from a possible non-abelian fractional quantum hall state,” *Phys. Rev. Lett.* **94**, 1–4 (2005), arXiv:0412343 [cond-mat].
- ³⁶A. Stern and B. I. Halperin, “Proposed Experiments to Probe the Non-Abelian $\nu=5/2$ Quantum Hall State,” *Phys. Rev. Lett.* **96**, 016802 (2006), arXiv:0508447 [cond-mat].
- ³⁷P. Bonderson, A. Kitaev, and K. Shtengel, “Detecting Non-Abelian Statistics in the $\nu=5/2$ Fractional Quantum Hall State,” *Phys. Rev. Lett.* **96**, 016803 (2006), arXiv:0508616 [cond-mat].
- ³⁸D. E. Feldman, Y. Gefen, A. Kitaev, K. T. Law, and A. Stern, “Shot noise in an anyonic Mach-Zehnder interferometer,” *Phys. Rev. B - Condens. Matter Mater. Phys.* **76**, 1–9 (2007), arXiv:0612608 [cond-mat].
- ³⁹A. Hofmann, V. F. Maisi, C. Gold, T. Krähenmann, C. Rössler, J. Basset, P. Märki, C. Reichl, W. Wegscheider, K. Ensslin, and T. Ihn, “Measuring the degeneracy of discrete energy levels using a GaAs/AlGaAs quantum dot,” *Phys. Rev. Lett.* **117**, 1–6 (2016), arXiv:1610.00928.
- ⁴⁰A. Harzheim, J. K. Sowa, J. L. Swett, G. A. D. Briggs, J. A. Mol, and P. Gehring, “Role of metallic leads and electronic degeneracies in thermoelectric power generation in quantum dots,” *Phys. Rev. Res.* **2**, 013140 (2020), arXiv:1906.05401.
- ⁴¹Y. V. Nazarov and Y. M. Blanter, *Quantum Transport* (Cambridge University Press, Cambridge, 2009).
- ⁴²R. Hanson, L. P. Kouwenhoven, J. R. Petta, S. Tarucha, and L. M. Vandersypen, “Spins in few-electron quantum dots,” *Rev. Mod. Phys.* **79**, 1217–1265 (2007), arXiv:0610433 [cond-mat].
- ⁴³J. M. Thijssen and H. S. J. Van der Zant, “Charge transport and single-electron effects in nanoscale systems,” *Phys. status solidi* **245**, 1455–1470 (2008).
- ⁴⁴E. A. Osorio, T. Bjørnholm, J. M. Lehn, M. Ruben, and H. S. Van Der Zant, “Single-molecule transport in three-terminal devices,” *J. Phys. Condens. Matter* **20** (2008), 10.1088/0953-8984/20/37/374121.
- ⁴⁵C. Brooke, A. Vezzoli, S. J. Higgins, L. A. Zotti, J. J. Palacios, and R. J. Nichols, “Resonant transport and electrostatic effects in single-molecule electrical junctions,” *Phys. Rev. B - Condens. Matter Mater. Phys.* **91**, 1–9 (2015).
- ⁴⁶C. W. J. Beenakker, “Theory of Coulomb-blockade oscillations in the conductance of a quantum dot,” *Phys. Rev. B* **44**, 1646–1656 (1991).
- ⁴⁷Y. Kim, W. Jeong, K. Kim, W. Lee, and P. Reddy, “Electrostatic control of thermoelectricity in molecular junctions,” *Nat. Nanotechnol.* **9**, 881–885 (2014).
- ⁴⁸J. O. Thomas, B. Limburg, J. K. Sowa, K. Willick, J. Baugh, G. A. D. Briggs, E. M. Gauger, H. L. Anderson, and J. A. Mol, “Understanding resonant charge transport through weakly coupled single-molecule junctions,” *Nature Communications* **10**, 4628 (2019).
- ⁴⁹J. K. Sowa, J. A. Mol, and E. M. Gauger, “Marcus Theory of Thermoelectricity in Molecular Junctions,” *J. Phys. Chem. C* **123**, 4103–4108 (2019).
- ⁵⁰A. Beckel, A. Kurzman, M. Geller, A. Ludwig, A. D. Wieck, J. König, and A. Lorke, “Asymmetry of charge relaxation times in quantum dots: The influence of degeneracy,” *Epl* **106** (2014), 10.1209/0295-5075/106/47002, arXiv:1402.5908.
- ⁵¹R. Scheibner, H. Buhmann, D. Reuter, M. N. Kiselev, and L. W. Molenkamp, “Thermopower of a kondo spin-correlated quantum dot,” *Phys. Rev. Lett.* **95**, 1–4 (2005), arXiv:0410671 [cond-mat].
- ⁵²A. Svilans, M. Josefsson, A. M. Burke, S. Fahlvik, C. Thelander, H. Linke, and M. Leijnse, “Thermoelectric Characterization of the Kondo Resonance in Nanowire Quantum Dots,” *Phys. Rev. Lett.* **121**, 206801 (2018), arXiv:1807.07807.
- ⁵³S. J. Blundell and K. M. Blundell, *Concepts in Thermal Physics* (Oxford University Press, 2009).
- ⁵⁴I. Ford, *Statistical Physics: An Entropic Approach* (John Wiley & Sons, Ltd, Chichester, UK, 2013).
- ⁵⁵T. Child, O. Sheekey, S. Lüscher, S. Fallahi, G. C. Gardner, M. Manfra, Y. Kleorin, Y. Meir, and J. Folk, “Entropy measurement of a strongly correlated quantum dot,” (2021), arXiv:2110.14158.
- ⁵⁶E. Sela, Y. Oreg, S. Plugge, N. Hartman, S. Lüscher, and J. Folk, “Detecting the universal fractional entropy of majorana zero modes,” *Phys. Rev. Lett.* **123**, 147702 (2019).
- ⁵⁷T. Child, O. Sheekey, S. Lüscher, S. Fallahi, G. C. Gardner, M. Manfra, and J. Folk, “A robust protocol for entropy measurement in mesoscopic circuits,” , 1–7 (2021), arXiv:2110.14172.
- ⁵⁸E. Pyurbeeva, C. Hsu, D. Vogel, C. Wegeberg, M. Mayor, H. Van Der Zant, J. A. Mol, and P. Gehring, “Controlling the Entropy of a Single-Molecule Junction,” *Nano Lett.* **21**, 9715–9719 (2021), arXiv:2109.06741.
- ⁵⁹J. S. Seldenthuis, H. S. J. van der Zant, M. A. Ratner, and J. M. Thijssen, “Vibrational excitations in weakly coupled single-molecule junctions: A computational analysis,” *ACS Nano* **2**, 1445–1451 (2008), <https://doi.org/10.1021/nn800170h>.
- ⁶⁰A. Kitaev, “Fault-tolerant quantum computation by anyons,” *Annals of Physics* **303**, 2–30 (2003).
- ⁶¹B. Lian, X.-Q. Sun, A. Vaezi, X.-L. Qi, and S.-C. Zhang, “Topological quantum computation based on chiral majorana fermions,” *Proceedings of the National Academy of Sciences* **115**, 10938–10942 (2018), <https://www.pnas.org/doi/pdf/10.1073/pnas.1810003115>.
- ⁶²H. H. Thorp, “Editorial expression of concern,” *Science* **374**, 1454–1454 (2021), <https://www.science.org/doi/pdf/10.1126/science.abn5849>.
- ⁶³M. Kayyalha, D. Xiao, R. Zhang, J. Shin, J. Jiang, F. Wang, Y.-F. Zhao, R. Xiao, L. Zhang, K. M. Fijalkowski, P. Mandal, M. Winnerlein, C. Gould, Q. Li, L. W. Molenkamp, M. H. W. Chan, N. Samarth, and C.-Z. Chang, “Absence of evidence for chiral majorana modes in quantum anomalous hall-superconductor devices,” *Science* **367**, 64–67 (2020), <https://www.science.org/doi/pdf/10.1126/science.aax6361>.
- ⁶⁴H. Zhang, C.-X. Liu, S. Gazibegovic, D. Xu, J. A. Logan, G. Wang, N. van Loo, J. D. S. Bommer, M. W. A. de Moor, D. Car, R. L. M. Op het Veld, P. J. van Veldhoven, S. Koelling, M. A. Verheijen, M. Pendharkar, D. J. Pennachio, B. Shojaei, J. S. Lee, C. J. Palmström, E. P. A. M. Bakkers, S. Das Sarma, and L. P. Kouwenhoven, “Retraction note: Quantized majorana conductance,” *Nature* **591**, E30–E30 (2021).
- ⁶⁵J. Sills and H. H. Thorp, “Editorial expression of concern,” *Science* **373**, 500–500 (2021), <https://www.science.org/doi/pdf/10.1126/science.abl5286>.
- ⁶⁶G. Ben-Shach, C. R. Laumann, I. Neder, A. Yacoby, and B. I. Halperin, “Detecting non-abelian anyons by charging spectroscopy,” *Phys. Rev. Lett.* **110**, 106805 (2013).
- ⁶⁷S. Smirnov, “Majorana tunneling entropy,” *Phys. Rev. B* **92**, 195312 (2015).
- ⁶⁸S. Smirnov, “Majorana entropy revival via tunneling phases,” *Phys. Rev. B* **103**, 075440 (2021).
- ⁶⁹M. Gau, R. Egger, A. Zazunov, and Y. Gefen, “Towards dark space stabilization and manipulation in driven dissipative majorana platforms,” *Phys. Rev. B* **102**, 134501 (2020).
- ⁷⁰M. Gau, R. Egger, A. Zazunov, and Y. Gefen, “Driven dissipative majorana dark spaces,” *Phys. Rev. Lett.* **125**, 147701 (2020).
- ⁷¹S. Smirnov, “Majorana ensembles with fractional entropy and conductance in nanoscopic systems,” *Phys. Rev. B* **104**, 205406 (2021).
- ⁷²C. Hsu, T. A. Costi, D. Vogel, C. Wegeberg, M. Mayor, H. S. J. van der Zant, and P. Gehring, “Magnetic-field universality of the kondo effect revealed by thermocurrent spectroscopy,” *Phys. Rev. Lett.* **128**, 147701 (2022).
- ⁷³Z. Iftikhar, S. Jezouin, A. Anthore, U. Gennser, F. D. Parmentier, A. Cavanna, and F. Pierre, “Two-channel kondo effect and renormalization flow with macroscopic quantum charge states,” *Nature* **526**, 233–236 (2015).
- ⁷⁴Z. Iftikhar, A. Anthore, A. K. Mitchell, F. D. Parmentier, U. Gennser, A. Ouerghi, A. Cavanna, C. Mora, P. Simon, and F. Pierre, “Tunable quantum criticality and super-ballistic transport in a “charge” kondo circuit,” *Science* **360**, 1315–1320 (2018), <https://www.science.org/doi/pdf/10.1126/science.aan5592>.
- ⁷⁵U. Meirav, M. A. Kastner, and S. J. Wind, “Single-electron charging and periodic conductance resonances in gaas nanostructures,” *Phys. Rev. Lett.* **65**, 771–774 (1990).
- ⁷⁶M. A. Reed, J. N. Randall, R. J. Aggarwal, R. J. Matyi, T. M. Moore, and A. E. Wetsel, “Observation of discrete electronic states in a zero-dimensional semiconductor nanostructure,” *Phys. Rev. Lett.* **60**, 535–537 (1988).
- ⁷⁷C. Thelander, T. Mårtensson, M. T. Björk, B. J. Ohlsson, M. W. Larsson, L. R. Wallenberg, and L. Samuelson, “Single-electron transistors in heterostructure nanowires,” *Applied Physics Letters* **83**, 2052–2054 (2003), <https://doi.org/10.1063/1.1606889>.

- ⁷⁸W. Liang, M. P. Shores, M. Bockrath, J. R. Long, and H. Park, "Kondo resonance in a single-molecule transistor," *Nature* **417**, 725–729 (2002).
- ⁷⁹P. Gehring, J. M. Thijssen, and H. S. J. van der Zant, "Single-molecule quantum-transport phenomena in break junctions," *Nature Reviews Physics* **1**, 381–396 (2019).
- ⁸⁰P. Reddy, S.-Y. Jang, R. A. Segalman, and A. Majumdar, "Thermoelectricity in molecular junctions," *Science* **315**, 1568–1571 (2007), <https://www.science.org/doi/pdf/10.1126/science.1137149>.
- ⁸¹L. Rincón-García, C. Evangeli, G. Rubio-Bollinger, and N. Agrait, "Thermopower measurements in molecular junctions," *Chem. Soc. Rev.* **45**, 4285–4306 (2016).
- ⁸²L. Cui, R. Miao, C. Jiang, E. Meyhofer, and P. Reddy, "Perspective: Thermal and thermoelectric transport in molecular junctions," *The Journal of Chemical Physics* **146**, 092201 (2017), <https://doi.org/10.1063/1.4976982>.
- ⁸³P. Gehring, A. Harzheim, J. Spièce, Y. Sheng, G. Rogers, C. Evangeli, A. Mishra, B. J. Robinson, K. Porfyakis, J. H. Warner, O. V. Kolosov, G. A. D. Briggs, and J. A. Mol, "Field-effect control of graphene–fullerene thermoelectric nanodevices," *Nano Letters* **17**, 7055–7061 (2017), pMID: 28982009, <https://doi.org/10.1021/acs.nanolett.7b03736>.
- ⁸⁴K. Wang, E. Meyhofer, and P. Reddy, "Thermal and thermoelectric properties of molecular junctions," *Advanced Functional Materials* **30**, 1904534 (2020), <https://onlinelibrary.wiley.com/doi/pdf/10.1002/adfm.201904534>.
- ⁸⁵S. Park, S. Kang, and H. J. Yoon, "Power factor of one molecule thick films and length dependence," *ACS Central Science* **5**, 1975–1982 (2019), pMID: 31893227, <https://doi.org/10.1021/acscentsci.9b01042>.
- ⁸⁶J. R. Widawsky, P. Darancet, J. B. Neaton, and L. Venkataraman, "Simultaneous determination of conductance and thermopower of single molecule junctions," *Nano Letters* **12**, 354–358 (2012), pMID: 22128800, <https://doi.org/10.1021/nl203634m>.
- ⁸⁷C. J. Lambert, H. Sadeghi, and Q. H. Al-Galiby, "Quantum-interference-enhanced thermoelectricity in single molecules and molecular films," *Comptes Rendus Physique* **17**, 1084–1095 (2016), mesoscopic thermoelectric phenomena / Phénomènes thermoélectriques mésoscopiques.
- ⁸⁸S. Dorsch, S. Fahlvik, and A. Burke, "Characterization of electrostatically defined bottom-heated InAs nanowire quantum dot systems," *New J. Phys.* **23** (2021), 10.1088/1367-2630/ac434c.
- ⁸⁹K. Micadei, J. P. S. Peterson, A. M. Souza, R. S. Sarthour, I. S. Oliveira, G. T. Landi, T. B. Batalhão, R. M. Serra, and E. Lutz, "Reversing the direction of heat flow using quantum correlations," *Nat. Commun.* **10**, 2456 (2019), arXiv:1711.03323v1.